THE ASTROPHYSICAL JOURNAL, 291:72–79, 1985 April 1

IUE OBSERVATIONS OF A STARBURST DISK AND THE DETECTABILITY OF HIGH REDSHIFT GALAXIES

D. W. WEEDMAN[1] AND D. P. HUENEMOERDER
Department of Astronomy, Pennsylvania State University
Received 1984 June 18; accepted 1984 October 16

ABSTRACT

The high-surface-brightness inner disk of NGC 1068 has been observed with the *IUE* to determine the ultraviolet spectrum and surface brightness profile. This disk is explained by an intense starburst, requiring formation of 1–2 massive stars yr^{-1}, so it is a good prototype for seeking at early epochs in the universe. Calculations of isophotal diameter as a function of redshift are presented. It is found that this disk could be resolved to $z \approx 0.3$ from the ground or to $z \approx 2.0$ with the Hubble Space Telescope. For $z \gtrsim 1.3$, such a disk is more easily observable than a large, normal galaxy.

Subject headings: galaxies: individual — galaxies: photometry — galaxies: Seyfert — galaxies: stellar content — stars: formation — ultraviolet: spectra

I. INTRODUCTION

At some epoch in the universe, extensive star formation occurred that led to the galaxies seen today. An exciting motivation for increasing the sensitivity of optical and infrared observations is the attempt to track galactic evolution, initially by locating an epoch at which star formation was more widespread than at the present. Recent observations of faint, blue galaxies have given hope that such an epoch is observable (Butcher and Oemler 1978; Bruzual and Kron 1980). The difficulty in interpreting or anticipating such observations is the uncertainty regarding how these galaxies should appear. Not only are parameters related to star formation uncertain, but dust probably redistributes most ultraviolet radiation to the infrared, confusing attempts to predict the spectrum.

In the present paper, we provide an empirical comparison for seeking star-forming spiral galaxies at high redshift. This is done by using new ultraviolet observations of the disk of the brightest local example known; the appearance of an identical galaxy is then described as a function of redshift. The galaxy observed is NGC 1068; it has the further important property that far-infrared observations are available for the bright disk (Telesco *et al.* 1984), providing sufficient constraints when used with the ultraviolet and emission-line data that the parameters of star formation can be specified. This ties the data for NGC 1068 quantitatively to models for star formation in spiral galaxies.

The galaxy NGC 1068 is widely known as the prototype Seyfert 2 galaxy. Many studies have been undertaken of its nuclear properties. This galaxy has another distinguishing characteristic, a bright inner disk, about 50″ in diameter, of exceptionally high surface brightness. This disk is noticed by most observers of this galaxy (e.g. Sandage 1961). In the survey of Keel and Weedman (1978), it was found to have the highest surface brightness of any spiral galaxy seen. It is reasonable to presume that the disk in some way relates to the activity in the nucleus, but which of these has triggered the other is not known. For the present investigation, the importance of the disk is that its properties can be fully explained by widespread star formation, a phenomenon frequently described as a starburst. Being so bright, this disk provides a valuable upper extreme to the intensity of a starburst in a local spiral galaxy. In all that follows, the active nucleus of NGC 1068 is ignored.

[1] Guest Observer with the *International Ultraviolet Explorer* satellite, which is sponsored and operated by the National Aeronautics and Space Administration, the Science Research Council of the United Kingdom, and the European Space Agency.

II. OBSERVATIONS

Because our primary objective is to describe how this galactic disk would appear at high redshift, it is necessary to determine its spectrum and luminosity profile in the ultraviolet. The disk is sufficiently bright that we were able to accomplish this using the *International Ultraviolet Explorer satellite* (*IUE*). The *IUE* has been used several times to observe NGC 1068, with the intention of studying the nucleus (e.g., Neugebauer *et al.* 1980). It is possible, as reported below, to use two-dimensional data analysis on these archival observations to determine properties of the disk in the immediate vicinity of the nucleus. Our own observations were designed to obtain disk spectra substantially further away from the nucleus. To obtain such data, we devoted two *IUE* shifts to this disk. Details and positions of the new observations are given in Table 1 and Figure 1; archival exposures which we reanalyzed are also given in Table 1. A good example of the way in which the nuclear and disk spectra can be separated, even for observations that include both, is given by considering our observation SWP 21734. Using standard *IUE* processing techniques (Turnrose, Harvel, and Stone 1981), individual spectra are available for 15 lines corresponding to 15 positions down the long axis of the observing aperture (10″ × 22″). A "cut" through the spectrum at a given wavelength then gives a one-dimensional monochromatic profile of the object observed. Such a cut for image SWP 21734 is shown in Figure 2, illustrating for convenience both the image scale and the relative sensitivity along the aperture. From the position of this observation (Fig. 1), it might be expected that the brighter central lines arise from the nucleus. Indeed, the spectrum of just the central five lines, shown in Figure 3, shows the characteristic strong nuclear emission lines. But the spectrum of the remaining lines, in Figure 4, has no such emission, so we assume it to be a spectrum of the disk. The size scale (nucleus less than 10″ diameter) is what is expected from optical observations.

TABLE 1

IUE OBSERVATIONS OF NGC 1068

Observation	Date[a]	Exposure (min)	Location	Source
SWP 21734	1983 Dec 9 (83/343)	240	offset 5″ NE	new
SWP 21751	1983 Dec 12 (83/346)	430	offset 16″ SW	new
SWP 9355	1980 Jun 23 (80/175)	30	nucleus	archive
SWP 9356	1980 Jun 23 (80/175)	45	nucleus	archive
SWP 14360	1981 Jun 30 (81/181)	90	nucleus	archive
SWP 14589	1981 Jul 30 (81/211)	183	nucleus	archive
SWP 15856	1981 Dec 23 (81/357)	147	offset 12″	archive
SWP 16433	1982 Feb 26 (82/057)	30	nucleus	archive
SWP 17623	1982 Aug 7 (82/219)	150	offset 12″	archive
LWR 1666	1978 Jun 19 (78/165)	40	nucleus	archive
LWR 8115	1980 Jun 23 (80/175)	30	nucleus	archive
LWR 10969	1981 Jun 30 (81/181)	40	nucleus	archive
LWR 10970	1981 Jun 30 (81/181)	120	nucleus	archive
LWR 11186	1981 Jul 30 (81/211)	30	nucleus	archive

[a] Date as formatted in *IUE* log shown in parentheses.

Our objective is to determine the surface brightness profile of the disk in the ultraviolet. Consequently, it is necessary to determine surface brightness from the flux contained in a given number of lines in the spectrum. This is straightforward as long as it is assumed the portion of the disk observed is homogeneous. When the aperture is uncontaminated by the nucleus, so the entire spectrum is from the disk—as is the case for our observation SWP 21751 and archival observation SWP 14589—the response function of the aperture is accommodated by using an effective area of 200 arcsec^2 (Panek 1982). In other cases, we have to apply an effective area for each line included, as determined from slit response profiles of trailed stars (Cassatella, Barbero, and Benvenuti 1984). All the results we have deduced in this way are summarized in Table 2. Fluxes have been transformed to surface brightnesses, arbitrarily using wavelengths of 1280, 1890, 2200, 2600, and 3000 Å. Because the spectrum is very nearly flat throughout this range, there is no need to specify it at additional wavelengths. Uncertainty in the placement of the aperture proves to be the major source of uncertainty in these results. Calibration uncertainty or the low signal-to-noise ratio of some spectra are negligible effects by comparison. We adopted the effective radii listed in Table 2 just by examining the aperture placements shown in Figure 1; the *IUE* is not able to set more precisely than about $\pm 2''$, which can be considered the uncertainty in these positions. (Observations were made by first setting the *IUE* on the bright nucleus, easily acquired, and offsetting from that.)

All the archival spectra centered on the nucleus do show off-nucleus continuum. In all cases, however, this continuum is dominated by a bright knot off the nucleus; it happened that the aperture was at a position angle to include this for all observations (Snijders, Briggs, and Boksenberg 1982). In spectrum SWP 14589, this knot shows as a clear reversal in the profile along the slit. As this spectrum is bluer than the disk spectra well off the nucleus, we do not take the high surface brightness or spectrum of the knot as representative of the disk. The disk brightness profile and spectrum to be used are taken only from the off-nucleus observations. All available long wavelength data are also contaminated to some extent by the knot, because we have no off-nucleus LWR observations. The disk spectrum from 2000 Å to 3200 Å is flat, as it indeed must be to connect with the optical data described below, so it is safe

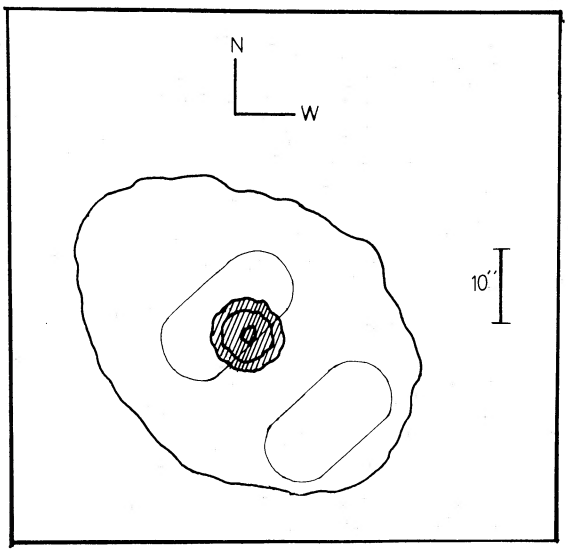

FIG. 1

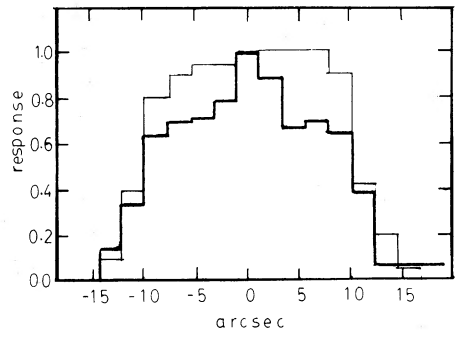

FIG. 2

FIG. 1.—Sketch of the bright disk and active nucleus of NGC 1068, showing positions of *IUE* aperture for observations SWP 21734 (*top*) and SWP 21751 (*bottom*).

FIG. 2.—*Dark line*: cut perpendicular to the spectrum showing flux distribution along aperture for observation SWP 21734. *Light line*: relative response function used to correct observed fluxes for position in aperture. Corresponding spatial scale shown on abscissa.

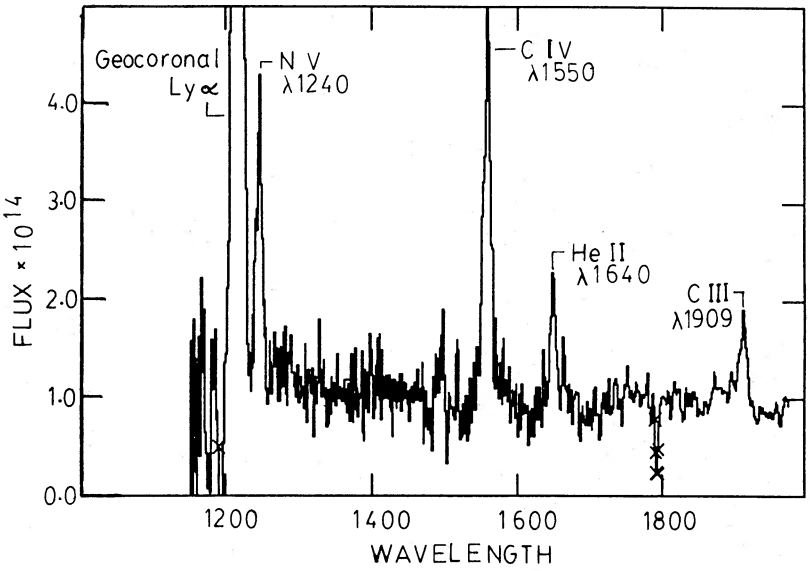

FIG. 3.—Spectrum of central five lines from cut in Fig. 2, showing characteristic nuclear emission spectrum

to adopt the shape of the LWR disk spectrum from the archival, on-nucleus data, but the normalization of this spectrum is determined by the off-nucleus SWP results.

Multiaperture *UBV* photometry of the disk by Smith, Weedman, and Spinrad (1972) provides surface brightnesses for optical wavelengths. These data, with apertures from 8".5 to 34" diameter, are used to determine average surface brightnesses in the annuli between apertures, using magnitude-to-flux transformations in Hayes and Latham (1975). Results are in Table 2.

III. THE DISK PROFILE AND STARBURST MODEL

The data in Table 2 will be used to fit the profile of an exponential disk, which will be assumed to represent the disk of NGC 1068. This disk profile will then be used to discuss the isophotal diameter of the disk as a function of redshift and detection limits. The notation to be used is:

- S_λ Observed surface brightness in ergs cm^{-2} s^{-1} Å^{-1} arcsec^{-2}
- λ Wavelength in the observer's frame
- λE Wavelength in the galaxy rest frame, $\lambda = \lambda E(1 + z)$
- $L_{\lambda E}$ Surface luminosity in ergs s^{-1} Å^{-1} pc^{-2} with wavelengths in the galaxy rest frame
- I_λ Central surface brightness of the exponential disk in ergs cm^{-2} s^{-1} Å^{-1} arcsec^{-2}
- r Observed angular radius on the disk, in arcsec
- a Scale size of the exponential disk, in arcsec
- A Scale size of the exponential disk, in kpc.

With this notation, the surface-brightness profile of an exponential disk is defined by $S_\lambda = I_\lambda \exp(-r/a)$. Parameters I_λ

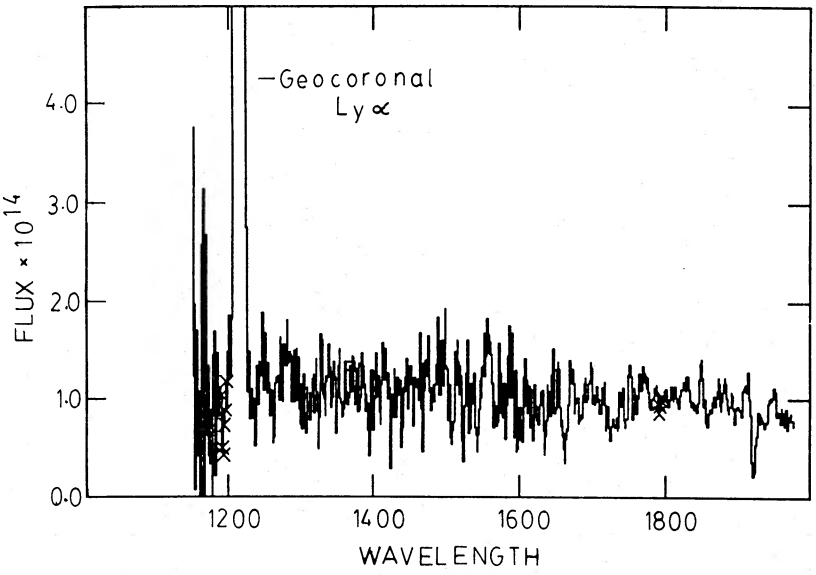

FIG. 4.—Spectrum of all lines other than central five from cut in Fig. 2, showing purely continuous spectrum of disk

TABLE 2

SURFACE BRIGHTNESSES OF NGC 1068 DISK[a]

A. ULTRAVIOLET

Observation	Effective Radius	S_{1280}	S_{1890}	S_{2200}	S_{2600}	S_{3000}
SWP 21734	8″	12	10	...	...	...
SWP 21751	17″	3.9	4.8	...	...	...
SWP 9355[b]	...	...	...	...	...	...
SWP 9356[b]	...	50	23	...	...	...
SWP 14360	...	33	22	...	...	...
SWP 14589	...	47	28	...	...	...
SWP 15856	...	6.0	6.5	...	...	...
SWP 16433	...	31	28	...	...	...
SWP 17623	...	3.0	4.0	...	...	...
LWR 1666	...	...	...	27	25	25
LWR 8115	...	...	...	23	21	21
LWR 10969	...	...	...	16	18	17
LWR 10970	...	...	...	16	16	17
LWR 11186	...	...	...	29	22	21

B. VISIBLE[a,c]

Aperture	Effective Radius	S_{3600}	S_{4400}	S_{5500}
16″.6 × 8″.5	6″.3	14	36	39
26″ × 16″.6	10″.6	9.2	22	21
34″ × 26″	15″	6.1	13	13

[a] Observed surface brightness values in units of 10^{-17} ergs cm^{-2} s^{-1} Å^{-1} arcsec^{-2}.

[b] Exposures 9355 and 9356 were co-added to give result listed.

[c] *UBV* magnitudes are assumed to have effective wavelengths 3600 Å, 4400 Å, 5500 Å and transformation: $U = -2.5 \log f_\lambda - 21.29$, $B = -2.5 \log f_\lambda - 20.42$, $V = -2.5 \log f_\lambda - 21.17$.

and a are determined empirically by the surface brightnesses in Table 2. First, a is determined for the five wavelengths that have surface brightness measures at different radii, giving a weighted average of $a = 9''.0$. Adopting this a, the I_λ are then calculated at these wavelengths with uncertainties determined using the scatter among I_λ deduced from different S_λ. The two archival *IUE* observations listed as offset by 12″ are not used in these calculations. While reasonably consistent with the results, the difference between them implies uncertainty in the actual offset positions. Having the I_λ at all wavelengths of interest is sufficient to describe the appearance of the disk as a function of redshift. The adopted continuous spectrum of the disk of NGC 1068 in units of I_λ is shown in Figure 5.

For comparison with models, it is useful to transform I_λ to surface luminosities that can be related to the starburst parameters. Using the infrared observations in Telesco *et al.* (1984) and comparing infrared surface brightnesses to those at other wavelengths, virtually all disk flux is in the infrared from 10 μm to 700 μm. This can be considered the bolometric flux. Telesco *et al.* present an infrared spectrum of the entire disk, and a surface brightness profile across the disk at 10 μm. Assuming a uniform disk spectrum and fitting the 10 μm profile to the exponential disk we have adopted, we find that the bolometric surface brightness at the disk center is 2.6×10^{-10} ergs cm^{-2} s^{-1} arcsec^{-2}, or a bolometric luminosity of 1.3×10^{39} ergs s^{-1} pc^{-2} ($cz = 1090$ km s^{-1} and $H_0 = 75$ km s^{-1} Mpc^{-1}). This is the extrapolated luminosity for the center of the fitted exponential disk; the observed infrared luminosity at the center of NGC 1068 is much brighter than this, being dominated by the Seyfert nucleus.

The exceptional infrared luminosity of the starburst disk is a demonstration that much radiation—presumably ultraviolet starlight from massive stars—is absorbed by dust, which reradiates in the infrared. The fact that the disk is visible in the ultraviolet demonstrates that some of this starlight escapes. Both the amount of dust extinction in the ultraviolet and the rate of star formation can be determined if we compare with starbursts having assumed forms of the initial mass function (IMF).

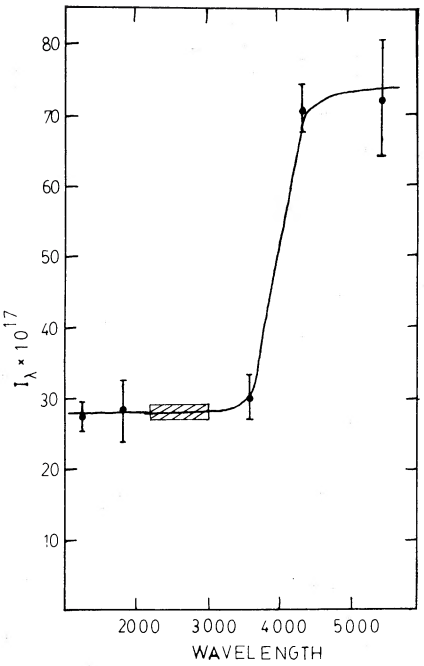

FIG. 5.—Central surface brightness I_λ for exponential disk in units of 10^{-17} ergs cm^{-2} s^{-1} Å^{-1} arcsec^{-2}. *Points and error bars*: values deduced from Table 2, as described in text. *Hatched rectangle*: values required from 2200 Å to 3000 Å to satisfy observation that LWP spectra are flat.

The relations described by Gehrz, Sramek, and Weedman (1983) should be valid for this situation. Those relations apply to an ongoing equilibrium starburst—one in which the lifetimes of individual massive stars are substantially less than the overall duration of the starburst. Because the results for NGC 1068 are averaged over the entire disk, incorporating star formation at various places, this approximation should be valid. This avoids the need for any parameter describing the lifetime of the star-forming episode.

Reviewing the necessary relations from Gehrz, Sramek, and Weedman, a steady state star-formation rate is given by $dN = N_0 m^{-\alpha} dM$, with dN and N_0 having units of number per unit time. The normalizing constant N_0 determines the absolute number of stars forming. Because stars are also dying, the number of stars present at any given time, denoted dP, is $dP = N_0 m^{-\alpha} \tau(m) dm$; $\tau(m)$ is the lifetime from Larson (1974).

The bolometric luminosity of the starburst is the total luminosity of all stars, so it is

$$L_{\rm bol} = \int_{m(l)}^{m(u)} l(m) dP \, .$$

By normalizing any model to $L_{\rm bol}$, the N_0 can be determined. The lower mass limit, m(l), and upper mass limit, m(u), are variable parameters for the starburst models, as is the index α. The bolometric luminosity as a function of mass, $l(m)$, is taken as tabulated in Table 3. These are deduced by combining results in Stothers (1972) and Kurucz (1979). From Stothers,

TABLE 3

LUMINOSITIES OF MASSIVE STARS

Mass ($M_\odot$)	$l(m)$[a]	$l_{1285}(m)$[b]
11.....	4	3.9
12.....	5	4.8
13.....	6.2	6.0
14.....	7.5	7.1
15.....	8.5	8.2
16.....	10	10
17.....	12	11
18.....	13	12
19.....	15	13
20.....	17	14
21.....	19	16
22.....	21	17
23.....	23	19
24.....	24	20
25.....	27	22
26.....	29	23
27.....	32	25
28.....	35	26
29.....	37	28
30.....	40	29
31.....	43	31
32.....	45	32
33.....	49	34
34.....	53	36
35.....	56	37
36.....	60	39
37.....	63	40
38.....	67	42
39.....	70	44
40.....	74	45
41.....	77	47
42.....	81	48
43.....	84	50
44.....	87	52
45.....	91	53
46.....	94	55
47.....	98	56
48.....	101	58
49.....	105	60
50.....	108	61

[a] Bolometric stellar luminosity in units of 10^{37} ergs s^{-1} using results in Stothers 1972 and Kurucz 1979.

[b] Monochromatic stellar luminosity at 1285 Å in units of 10^{34} ergs s^{-1} Å^{-1} using results in Stothers 1972 and Kurucz 1979.

the mean of three models of different composition for both zero-age main sequence and terminal-age main sequence is used to determine a relation between T_e and mass. Then, using Kurucz's atmosphere models (for $\log g = 4$), bolometric luminosity is found as a function of T_e. Combining these results gives the $l(m)$ in Table 3. Note that these are quite similar to the $l(m)$ assumed by Gehrz, Sramek, and Weedman even though they used different atmosphere models.

To determine extinction in the ultraviolet, we need to predict the unobscured ultraviolet continuum flux for the starburst. This is done for 1285 Å, one of the wavelengths at which Kurucz tabulated fluxes. The luminosity at 1285 Å, L_{1285}, is

$$L_{1285} = \int_{m(\mathrm{l})}^{m(\mathrm{u})} l_{1285}(m) dP \ .$$

The $l_{1285}(m)$ taken from Kurucz are also in Table 3.

Starburst models could be calculated for any values of m(l), m(u), and α. We present only two alternative models. One is weighted in favor of massive stars, with $m(\mathrm{l}) = 31$, $m(\mathrm{u}) = 50$, and $\alpha = 1.5$. Using the relations and units defined, this model gives $L_{\mathrm{bol}} N_0^{-1} = 2.35 \times 10^{44}$ and $L_{1285} N_0^{-1} = 1.46 \times 10^{41}$. The alternate is weighted to less massive stars, having $m(\mathrm{l}) = 11$, $m(\mathrm{u}) = 30$, and $\alpha = 2.5$. This model has $L_{\mathrm{bol}} N_0^{-1} = 1.79 \times 10^{43}$ and $L_{1285} N_0^{-1} = 1.54 \times 10^{40}$. The expected ratios of bolometric flux to flux at 1285 Å are 1.6×10^3 and 1.2×10^3 for these alternative models. Yet we observe a ratio of 10^6, taking the central bolometric surface brightness listed above (2.6×10^{-10} ergs cm^{-2} s^{-1} arcsec^{-2}) compared to that at 1285 Å in Figure 5 (27.5×10^{-17} ergs cm^{-2} s^{-1} Å^{-1} arcsec^{-2}). This means that less than 1% of the ultraviolet flux from the starburst is seen directly.

This result shows how the observed ultraviolet characteristics are extremely dependent on the amount and distribution of dust. A less obscured starburst would be a much brighter ultraviolet source. The fact that no brighter examples have been seen in spiral disks implies that most starbursts are even more shrouded than that in NGC 1068. The many *IRAS* sources with high infrared-to-optical flux ratios are examples (Soifer *et al.* 1984*a*, *b*). Even though only a very small fraction of the starburst luminosity for NGC 1068 leaks out in the ultraviolet and optical, it is sufficient to make the disk unusually conspicuous at those wavelengths.

Using the higher mass IMF model, the bolometric luminosity of NGC 1068 at the disk center requires stars to form at the rate of 0.5×10^{-6} yr^{-1} pc^{-2}, cycling mass at 16×10^{-6} $M_\odot$ yr^{-1} pc^{-2}. For the model with less massive stars, these requirements are 1.0×10^{-6} stars yr^{-1} pc^{-2} and 17×10^{-6} $M_\odot$ yr^{-1} pc^{-2}. To place these results in perspective, showing how extraordinary are such star formation rates, we can compare with the massive star formation rate near the Sun in our Galaxy. The formation rate given by Garmany, Conti, and Chiosi (1982) gives 1.2×10^{-10} $M_\odot$ yr^{-1} pc^{-2} for stars between 20 and 50 $M_\odot$ within 2.5 kpc of the Sun. This is only about 10^{-5} of the rate in the disk center of NGC 1068.

Integrating the two models over the exponential disk to a radius of 24″ gives total star formation rates of 0.8 or 1.9 yr^{-1}, with total mass cycling rates of 31 or 32 $M_\odot$ yr^{-1}. These values can be compared to other observed or theorized starbursts, to scale what we see in NGC 1068 to what might be expected elsewhere. Note that star birth rates are balanced by star death rates, so these numbers also give the number of supernovae yr^{-1} expected in the disk of NGC 1068.

IV. DETECTABILITY AT COSMOLOGICAL DISTANCES

Determining that a faint object is a galaxy requires that it be resolved. The detection itself, therefore, depends on the limiting surface brightness which the detecting instrument can reach. Effectively, determining whether a galaxy can be seen (as a galaxy) is equivalent to determining the isophotal diameter to the limiting detectable isophote, and then checking whether this diameter can be resolved with the detector used. Unfortunately, isophotal diameters depend in a complex way on the cosmology adopted and the intrinsic profile.

For nearby galaxies, at sufficiently small z for space to be Euclidean, the definition of isophotal diameter is straightforward. If the limiting isophote is S_λ (limit), the isophotal radius i'' is given by S_λ (limit) $= I_\lambda \exp(-i/a)$, for an exponential disk brightness profile. Under such circumstances, I_λ is independent of distance and a is determined by the ratio of physical scale

length A to distance. Significant modifications are necessary for cosmological distances (i.e., nonnegligible z).

Instead of remaining constant with distance, the surface brightness of a homogeneous disk decreases by five factors of $(1 + z)$. These include one factor for change in unit time, one for change in photon energy, one for change in bandpass, and two for change in unit area (i.e., the area corresponding to a pc^2 on the disk). Consequently, in a cosmologically useful relation for S_λ, the I_λ is $I_\lambda(z = 0)(1 + z)^{-5}$. It is the $I_\lambda(z = 0)$ that is displayed in Figure 5 for NGC 1068.

The scale size A is a metric quantity, so the analogous a will diminish with distance according to the relations for metric angular size; $a = 206265A(1 + z)/d$ for a in arcsec and d the proper distance. It is in the relation for d that a choice of cosmology must be made. We choose a Friedmann cosmology with $q_0 = 0.1$, which is deduced from estimates of the local density parameter $\Omega_0 = 2q_0$ (Davis and Peebles 1982). For this choice,

$$d = c\{10z - 90[(1 + 0.2z)^{1/2} - 1]\}H_0^{-1}(1 + z)^{-1}$$

(e.g., Sandage 1975). Assembling the concepts described, we find that the isophotal radius i'' for an exponential disk is given by

$$i = (1 + z)^2 \ln [(1 + z)^{-5}S_\lambda(\text{limit})^{-1}I_\lambda(z = 0)] \times (6.88 \times 10^{-4})H_0 A\{10z - 90[(1 + 0.2z)^{1/2} - 1]\}^{-1} .$$

Note that the ratio $S_\lambda(\text{limit})^{-1}I_\lambda(z = 0)$ is determined by specifying the limiting detectable isophote $S_\lambda(\text{limit})$ at the observer's wavelength λ, but using the I_λ read from Figure 5 at wavelength $\lambda(1 + z)^{-1}$. This procedure incorporates all terms normally referred to as a K-correction.

We can now proceed to determine the isophotal radius of the disk of NGC 1068 and thereby describe its detectability at high redshift. The only remaining parameter needed is $S_\lambda(\text{limit})$. Using CCD detectors, ground-based observations of galaxies have reported isophotes to a limit approximately 1% of the background sky surface brightness (e.g. Gehren *et al.* 1984; Kent 1984). This limit is about 26 mag arcsec^{-2}, or 8.5×10^{-20} ergs cm^{-2} s^{-1} Å^{-1} arcsec^{-2} at 6500 Å (an efficient wavelength for CCD detectors). This limit applies to galaxies large enough (diameter $\gtrsim 5''$) that many pixels provide the detection. It is not obvious just how to scale this limit as a galaxy becomes smaller in size, decreasing the number of illuminated pixels, because the scaling depends on the actual numbers of pixels required to define a detection. This is affected by various parameters, such as the ratio of seeing-limited resolution to pixel size and the ratio of sky brightness to detector background.

That the limit must be brighter for apparently small galaxies, near the seeing resolution limit, can be seen by considering the surface-brightness limit deduced from quoted detectability for unresolved objects. Observers with the most efficient detectors and ground-based telescopes uniformly report that under the very best conditions, with seeing images $\lesssim 1''$ diameter, it is possible to detect stellar-appearing objects of ~ 25 mag. The surface brightness of a $1''$ disk of 25th magnitude at 6500 Å is 2.7×10^{-19} ergs cm^{-2} s^{-1} Å^{-1} arcsec^{-2}, or 3 times brighter than the limit above for an extended source. Because $S_\lambda(\text{limit})$ is, therefore, a function of galaxy diameter, we calculate isophotal diameters with both values of $S_\lambda(\text{limit})$. The two results should bracket those for real galaxies, with the brighter limit being more realistic for small sources.

It is important to make similar determinations of $S_\lambda(\text{limit})$ for observations with the Hubble Space Telescope (HST), because searching for distant galaxies is a primary objective of this instrument. There are analogous uncertainties in picking the applicable $S_\lambda(\text{limit})$. Using the anticipated performance of the Wide Field Camera (WFC) reported by Westphal (1983), a single-orbit exposure will detect a stellar object of V magnitude 28.6 with signal-to-noise ratio of unity. This camera has pixel size of $0''.1$. Given the resolution capabilities, it is unlikely that an unresolved source will illuminate more than four pixels. This yields a lower limit to the detectable surface brightness of 3×10^{-19} ergs cm^{-2} s^{-1} Å^{-1} arcsec^{-2} at 5500 Å. The limit might be slightly fainter at 6500 Å because of the improved CCD detector efficiency. The signal-to-noise ratio achieved for detection of small extended sources should exceed unity, since more than four pixels would be illuminated. Because this limit is so close to one value deduced above for ground-based observations (2.7×10^{-19} ergs cm^{-2} s^{-1} Å^{-1} arcsec^{-2}), that same value will be used for convenience in the calculation to be illustrated. This similarity is not surprising, because the gain in performance by HST is meant to be primarily in resolution, i.e., the ability to determine whether a source of size $\lesssim 1''$ is a galaxy or not.

The Faint Object Camera (FOC) may prove to be the preferred instrument for determining if small sources are extended, because of its higher spatial resolution. Surface-brightness detection limits in the U band (3500 Å) are given by Machetto *et al.* (1983). For the f/48 camera, a single orbit exposure (taken as 5000 s) would give a signal-to-noise ratio of unity for an extended source of 26 mag arcsec^{-2}, or 1.2×10^{-19} ergs cm^{-2} s^{-1} Å^{-1} arcsec^{-2} at 3500 Å. Because of the detector, sensitivity drops off rapidly to the red, implying a surface brightness limit brighter than that for the WFC redward of 5500 Å. We present a calculation for U band observations of a starburst disk with the FOC using the limit quoted.

V. DISCUSSION AND CONCLUSIONS

Using all the parameters that have now been defined and determined, we show in Figure 6 the isophotal diameter ($2i''$) for a starburst disk like that in NGC 1068 as a function of redshift. Envelopes defined by different surface-brightness limits are given for ground-based observations at effective wavelength 6500 Å, optimized for existing CCD detectors, but they would change little at any other visible wavelength. This is because, at most redshifts of interest, the $I_\lambda(z = 0)$ arises from the flat, ultraviolet portion of the observed spectrum in Figure 5. Curves are also given for a 3500 Å observation with the FOC and a 6500 Å observation with the WFC on HST.

The results in Figure 6 illustrate our primary conclusions. Ground-based observations (assuming resolution limit of $2''$ to define the minimum detectable diameter of a galaxy) cannot resolve the starburst disk beyond $z = 0.4$. For HST, assuming a resolution limit of $0''.3$, slightly larger than the four pixels taken to define an unresolved source with the WFC, this disk could be resolved to $z = 1.7$. If the FOC can push resolution below $0''.2$, the disk could be resolved to $z > 2.4$. Recall that the disk of NGC 1068 provides an upper extreme to the disk brightness found for local spirals, so the applicable curve in Figure 6 is an optimistic case, if we scale only from known, local galaxies. As discussed in § III, however, the disk brightness depends critically on the amount of dust absorption, so less dusty disks could be much brighter. Also, the isophotal diameter scales directly with physical size A, so any increase in

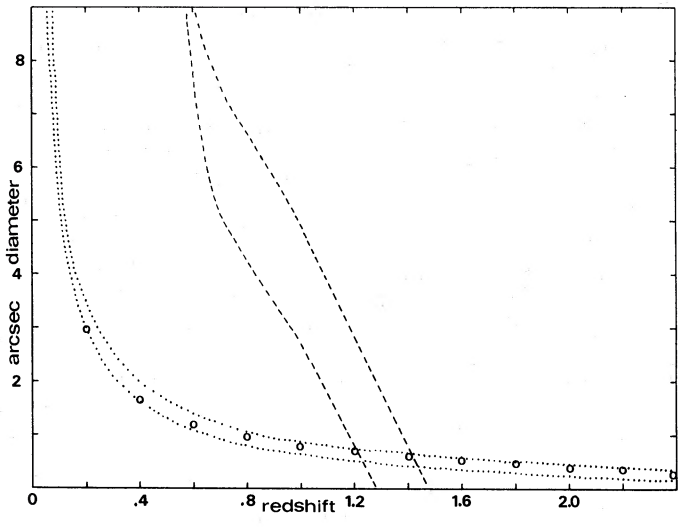

FIG. 6.—*Dotted envelope*: isophotal diameter of starburst disk like NGC 1068 for range of limiting surface brightness discussed in text for ground-based observations. Lower curve of this envelope also applies for observations with the WFC on Hubble Space Telescope. *Dashed envelope*: isophotal diameter of early-type spiral galaxy having scale size 6.3 kpc and central ultraviolet surface brightness like M31. Envelope encompasses range of limiting surface brightness discussed in text for ground-based observations. Lower curve of envelope also applies for observations with the WFC. *Open circles*: isophotal diameter of starburst disk like NGC 1068 for observation with FOC on Hubble Space Telescope.

A substantially increases the redshift limit, especially for an HST detection. Doubling the scale length A would push the WFC redshift limit to $z = 2.3$, but only increase the ground-based limit to $z = 0.8$.

The starburst disk of NGC 1068 is small compared to the overall extent of large spiral or elliptical galaxies (the scale length A for the exponential disk in NGC is only 0.63 kpc). It might then be expected that it is not a valid example for detecting at high redshifts. At first glance, this suspicion is confirmed by observations of the host galaxies of quasars, which are good examples of detection limits (Gehren *et al.* 1984, Hutchings *et al.* 1982). Galaxies have been found at $z \approx 0.5$ with isophotal diameters ~ 10 times what we calculate for the NGC 1068 starburst disk at this redshift. The explanation is that the starburst does not fill the entire disk. Even NGC 1068 has a much larger but fainter outer disk that resembles that in normal galaxies. At low redshifts (so that the ultraviolet continuum is not being observed), such disks define the isophotal diameter. At larger redshifts, especially once the rest frame wavelength falls below 4000 Å, the surface brightness of ordinary galaxies plummets.

To illustrate these effects quantitatively, we consider a galaxy having an exponential disk with a scale factor 10 times that of NGC 1068, but having central surface brightness like M31. The galaxy M31 is chosen as a comparison because it is an early-type spiral for which central surface brightness has been measured in the ultraviolet with absolute spatial resolution comparable to what we have for NGC 1068. The results are given by Coleman, Wu, and Weedman (1980) from the 2.5 aperture of the *Astronomical Netherlands Satellite*; this aperture would be analogous in subtended size to 7″ were M31 at the distance of NGC 1068. Central surface brightness I_λ for 1500 Å $< \lambda <$ 2500 Å is 0.5×10^{-17} ergs cm^{-2} s^{-1} Å^{-1} arcsec^{-2} in M31, or over 50 times fainter than for NGC 1068. Scaling the central surface brightness with wavelength according to the spectral energy distribution in Table 2 of Coleman, Wu, and Weedman, we can produce an $I_\lambda(z = 0)$ spectrum for M31 analogous to that in Figure 5 for NGC 1068. Using this with an exponential scale length $A = 6.3$ kpc, the isophotal diameter of a large spiral galaxy is calculated in the same way as done for the NGC 1068 disk. The result is also in Figure 6, and is an important comparison.

The normal disk is easily resolved at redshifts $\lesssim 1.0$, in agreement with observations. For a galaxy like NGC 1068, having a starburst embedded within a normal disk, the starburst would not determine the isophotal diameter until $z \gtrsim 1.3$. Near that redshift, the normal disk quickly disappears even though it remained above the ground-based limit to $z \approx 1.0$. Because the isophotal diameter of normal galaxies decreases so quickly with redshift, little improvement in the redshift limit at which they are resolvable is expected with HST. (All the quoted redshift limits for normal galaxies would be even less if an observing wavelength shortward of 6500 Å were used.) The curves in Figure 6 imply that the presence of extensive star-forming regions is necessary if we hope to resolve any galaxies at $z \gtrsim 1.3$, even with HST. While these results for NGC 1068 provide a benchmark scaled from a bright local spiral, what we hope to learn is how the early universe differed from the present epoch. If spiral galaxies at high redshift are found more easily than predicted by Figure 6, empirical evidence for evolution of spiral galaxies will have been seen.

We thank our observing assistant R. Pitts, and R. Thompson and the Goddard Regional Data Analysis Facility staff for help in making and analyzing the *IUE* observations. Also, we thank G. Rieke for useful comments. This research was supported by NASA grant NAG 5-334 and, in part, by NSF grant AST 8101204 to Pennsylvania State University.

REFERENCES

Bruzual, A. G., and Kron, R. G., 1980, *Ap. J.*, **241**, 25.
Butcher, H., and Oemler, A., Jr. 1978, *Ap. J.*, **219**, 18.
Cassatella, A., Barbero, J., and Benvenuti, P. 1984, in Report to 3 Agency (NASA, ESA, SERC) meeting held October 1983, CSC/TM-84/6042, p. A-150.
Coleman, G. D., Wu, C.-C., and Weedman, D. W. 1980, *Ap. J. Suppl.*, **43**, 393.
Davis, M., and Peebles, P. J. E. 1982, *Ap. J.*, **267**, 465.
Garmany, C. D., Conti, P. S., and Chiosi, C. 1982, *Ap. J.*, **263**, 777.
Gehren, T., Fried, J., Wehinger, P. A., and Wyckoff, S. 1984, *Ap. J.*, **278**, 11.
Gehrz, R. D., Sramek, R. A., and Weedman, D. W. 1983, *Ap. J.*, **267**, 551.
Hayes, D. S., and Latham, D. W. 1975, *Ap. J.*, **197**, 593.
Hutchings, J. B., Crampton, D., Campbell, B., Gower, A. C., and Morris, S. C. 1982, *Ap. J.*, **262**, 48.
Keel, W. C., and Weedman, D. W. 1978, *A.J.*, **83**, 1.
Kent, S. M. 1984, *Ap. J. Suppl.*, **56**, 105.
Kurucz, R. L. 1979, *Ap. J. Suppl.*, **40**, 1.
Larson, R. B. 1974, *M.N.R.A.S.*, **166**, 585.
Macchetto, F., *et al.* 1983, in *The Space Telescope Observatory*, ed. D. N. B. Hall (Greenbelt, MD: NASA), p. 40.
Neugebauer, G., *et al.* 1980, *Ap. J.*, **238**, 502.
Panek, R. J. 1982, *International Ultraviolet Explorer NASA Newsl.*, No. 18, p. 68.
Sandage, A. 1961, *The Hubble Atlas of Galaxies* (Washington: Carnegie Institution) p. 16.
———. 1975, in *Stars and Stellar Systems*, Vol. **9**, *Galaxies and the Universe*, ed. A. Sandage, M. Sandage, and J. Kristian (Chicago: University of Chicago Press), p. 761.
Smith, M. G., Weedman, D. W., and Spinrad, H. 1972, *Ap. Letters*, **11**, 21.

Snijders, M. A. J., Briggs, S. A., and Boksenberg, A. 1982, *Proc. 3 European IUE Conf.*, ed. E. Rolfe, A. Heck, and B. Battrick (Madrid: ESA), p. 551.
Soifer, B. T., *et al.* 1984*a*, *Ap. J.* (*Letters*), **278**, L71.
———. 1984*b*, *Ap. J.* (*Letters*), **283**, L1.
Stothers, R. 1972, *Ap. J.*, **175**, 431.
Telesco, C. M., Becklin, E. E., Wynn-Williams, C. G., and Harper, D. A. 1984, *Ap. J.*, **282**, 427.
Turnrose, B. E., Harvel, C. A., and Stone, D. F. 1981, *International Ultraviolet Explorer Image Processing Information Manual Version 1.1* (Greenbelt, MD: Computer Sciences Corp.).
Westphal, J. A. 1983, in *The Space Telescope Observatory*, ed. D. N. B. Hall (Greenbelt, MD: NASA), p. 28.

D. P. HUENEMOERDER and D. W. WEEDMAN: Department of Astronomy, 525 Davey Laboratory, Pennsylvania State University, University Park, PA 16802